Performance Evaluation of Remote Monitoring
Car-like Mobile Robot System with Grey Prediction Model

Mingcan Xu and Tao Huang[*]

Chongqing Three Gorges Vocational College, Chongqing 404155, China

Path planning has always been a hot research topic in various sensor applications of car-like mobile robots (CLMRs). In a known or unknown map information environment, a safe collision-free path of a CLMR from the starting point to the endpoint is planned according to strict indexes such as the shortest time and distance and the lowest energy consumption. To minimize the additional delay caused by the time-delay system in a remote sensing CLMR, a new predictive control algorithm is proposed for use in nonvisual environments. On the basis of the dynamic analysis and remote sensing model of the CLMR, the Smith predictor is used to compensate for the signal delay between the PHANTOM Omni controller and the CLMR, and reduce the positioning error caused by the delay. The grey prediction (GP) model is used to predict the values of the sensors on the CLMR and reduce the remote-control disoperation due to the delay. The feasibility of the GP algorithm is demonstrated by simulation, and a control experiment of force feedback between the PHANTOM Omni controller and a CLMR in a nonvisual environment demonstrated the feasibility of the system. The compensation effect was clearly shown, despite the experiments being performed by remote control with manipulators.

1. Introduction

Modern industrial production control is often accompanied by a time-delay system, which makes the system unable to accurately track its input. Moreover, once the system is affected by external interference, the overshoot of the system will gradually increase, affecting its stability. Serious overshoot can even endanger the safety of equipment and personnel. Therefore, compensating for the delay effect is an important topic in the field of car-like mobile robots (CLMRs) and also a research focus in the military, aviation, ocean, and power generation fields.[1]

In recent years, the theoretical research and practical application of the Smith predictor in modern industrial production processes have made remarkable progress.[2,3] To solve the delay problem in principle, Kirtania and Choudhury proposed a predictive controller with long dead times and designed a delay compensation device so that there was no lag between the output of

the controller and that of the system.[4] In other words, the Smith predictor can compensate for the delay of the controlled object and add a predictive compensation device in the closed-loop feedback loop. By adjusting the compensation device, the delay factor in the transfer function of the control object can be effectively isolated to improve the stability of the system and avoid large overruns.[5] In addition, the grey prediction (GP) model is at the core of grey system theory, which mainly consists of a generation function and grey differential equation, in which the basis is the grey generation function and the modeling method is differential fitting.[6] The solution of the grey quantity of the prediction model is to find patterns in the chaotic raw data, rather than to seek its statistical law and probability distribution. The basic idea is to process the original data into a regular data series and finally establish a GP model. The core of the GP model is the GM (1,1) model,[7] which can carry out modeling and prediction with a small amount of known information and has been extended to many practical prediction models.

To resolve the above problems, in this paper, we propose a new system to control CLMRs in a nonvisual environment. Then the Smith predictor is applied to compensate for the signal delay between the manipulator and the CLMR. Next, the GP model is used to predict the value obtained by the CLMR sensors to reduce the remote-control disoperation caused by the time delay. Finally, the feasibility of the algorithm and system is demonstrated by simulation experiments.

2. Related Works

CLMRs are gradually having an increasing effect on people's daily lives. In the CLMR field, path planning, which can be divided into global and local path planning, has always been a hot research topic. The common global path planning algorithms include raster-based methods,[8] sampling-based methods,[9] and some intelligent algorithms.[10] Such algorithms are usually based on accurate global maps, which are often difficult to grasp in advance in real situations. The local path planning algorithm refers to the real-time planning of a CLMR according to the data of various sensors (e.g., 2D lidar [11] and camera [12]), which can better adapt to the unknown working environment.

Considerable research has been carried out on full traversal path planning CLMRs.[13,14] The progress in research on applying CLMRs to the manufacturing industry has been remarkable. In particular, the United States and Japan first introduced CLMRs, and the United States formulated a strategic plan for a ground space–human combat platform, which was the prelude to research on CLMRs in the early 1980s. In addition to CLMR research, Japan will also focus on middleware research in the future. China is also performing increasing research on CLMR, and the development of CLMR technology has long been regarded as an important development field of robot research. The traditional ant colony optimization algorithm (ACO) applies a weight matrix to form a connection relationship between the shortest path and obstacles in the range of activity of a CLMR and optimize the spatial distance of each element to obtain path planning results. Although the traditional ACO considers obstacles and other problems that affect the path distance, it has the disadvantages of slow convergence and easy trapping at local optima. To solve the problems encountered by an CLMR in path planning, Hwang and Chang proposed a

path planning algorithm for hexapod robots facing unknown maps.[15] In this algorithm, the shape of the obstacle is classified by ranging group and fuzzy rules, an environmental map is built, a modified repulsive function is introduced, and local path planning is carried out by the artificial potential field method. The simulation results show that the path planning method has high feasibility, but it does not fully consider the impact of a full traversal environment, resulting in a long path planning process. Majd *et al.* proposed a CLMR path planning method based on arc-linear-arc theory according to double-arc theory, and a tracked mobile platform was used to experimentally verify this method in a laboratory environment.[16] The experimental results showed that the mean values of the lateral error and longitudinal error in path planning are low, which indicates that the method is effective for applications, but it cannot effectively obtain the optimal path. To better maintain a formation of CLMRs, Rathinam *et al.* transformed the formation control problem into a trajectory tracking problem. According to the position of each CLMR in the formation, trajectory parameters were calculated separately, and a formation of CLMRs was controlled on the dynamic level, although no research related to dynamic coordination and dynamic control was conducted.[17] To sum up, the pilot-follow method,[18] virtual structure method,[19] and behavior-based method[20] are often adopted in research on the control of CLMR formations. On the other hand, owing to external factors such as weather, the pilot speed and workshop distance must be constantly adjusted during formation planning. The above method must constantly calculate and update the track parameters used to follow the CLMRs, which increases the calculation burden of the system, causes instability, and reduces the practicality of the system.

With the above background, a remote-control system of a CLMR based on a predictive algorithm for local path planning is proposed in this paper. To reduce the positioning error caused by the additional delay, the Smith predictor is used to compensate for the additional delay between a PHANTOM Omni controller and the CLMR. At the same time, to reduce the disoperation caused by the additional delay, the GP model is used to predict the values of sensors on the CLMR.

3. Controller and CLMR Modeling

The haptic device PHANTOM Omni from US Sensible Technologies serves as the controller in the GP control algorithm. After the remote monitoring system is started, the manipulator controls the CLMR by operating the interactive PHANTOM Omni device. According to the position relationship of the interaction process, the position attitude of the CLMR is collected to determine whether a collision has occurred. If a collision has occurred, the PHANTOM Omni controller is triggered and the collision force is calculated using the collision data. The controller then moves the handle of the force feedback device to the correct location, then holds down the button to control the CLMR, and releases the button to stop control. If other objects (such as obstructions) are added to the environment, the manipulator can also simulate the environment force (contact force, gravity, friction force, spring force, etc.) to "feel" the pilot. If the actual CLMR is equipped with mechanical sensors, the PHANTOM Omni controls the CLMR and can also read the mechanical information and feed it back to the manipulator.

3.1 Structural modeling of PHANTOM Omni controller

The general kinetic equation of the one-degree-of-freedom CLMR is

$$M(q)q'' + C(q, q')q' + d + G(q) = \tau, \tag{1}$$

where $q \in R^n$ is the joint rotation angle, q' is the angular velocity of the CLMR, q'' is the angular acceleration of the CLMR, $M(q)$ is an $n \times n$ positive definite inertia matrix, $C(q, q')$ is a matrix comprising the Coriolis force and centrifugal force terms, $G(q)$ is the gravity term, d is the external interference, and $\tau \in R^n$ is the torque vector of each joint of the CLMR, namely, the control input. The dynamic model of the CLMR has the following characteristics: the inertia matrix $M(q)$ is symmetric positive definite and bounded, and a skew-symmetric matrix $M(q) - 2C(q, q')$, namely, $X^T(M(q) - 2C(q, q')) = 0$, exists for any vector X. The PHANTOM Omni controller studied in this paper is shown in Fig. 1.

The PHANTOM Omni CLMR has three rotating joints q_1, q_2, and q_3. Its inertia matrix $M(q)$ is the 3×3 matrix

$$M(q) = \begin{bmatrix} M_{11} & M_{12} & 0 \\ M_{21} & M_{22} & M_{23} \\ 0 & M_{32} & M_{33} \end{bmatrix}, \tag{2}$$

where $M_{12} = M_{21} = a_7\cos(q_2)$, $M_{23} = M_{32} = -0.5a_5\sin(q_2 - q_3) + 0.5a_6\cos(q_2 - q_3)$, $M_{11} = a_1 + a_2\cos(2q_2) + a_3\cos(2q_3) + a_4\cos(2q_3) + a_5\cos(q_2)\sin(q_3) + a_6\cos(q_2)\sin(q_3)$, $M_{22} = a_8$, and $M_{33} = a_9$ exist. Here, a_1, a_2, ..., a_9 are constants greater than 0. The combined vector of the Coriolis force, the centrifugal force terms, and the gravity term is
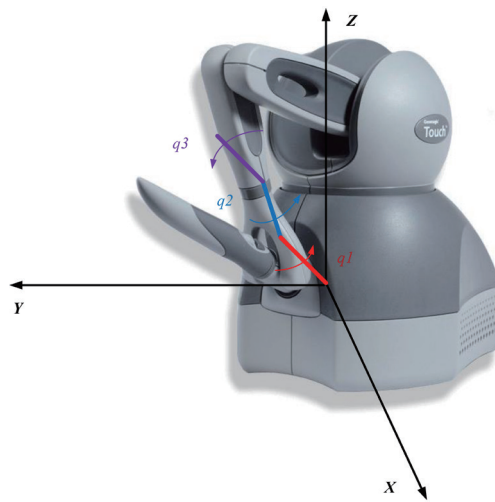
Fig. 1.   (Color online) Architecture of PHANTOM Omni controller.

$$V(q, q') = [V_1, V_2, V_3]^T = C(q, q')q' + G(q). \tag{3}$$

Since the movement of the second and third joints is on the same horizontal plane, to simplify the operation, the second joint is locked in this study, and only the angle variables q_1 and q_3 of the first and third joints are considered for analysis and research. At this point, corresponding to Eq. (2), the specific expressions of each matrix and vector in the PHANTOM Omni CLMR are as follows:

$$M(q) = \begin{bmatrix} a_1 + a_2 c_{2,3} + a_3 s_{2,3} + a_4 c_3 + a_5 s_3 & 0 \\ 0 & a_6 \end{bmatrix}, \tag{4}$$

where $c_i = \cos(q_i)$, $s_i = \sin(q_i)$, $c_{2,i} = \cos(2q_i)$, and $s_{2,i} = \sin(2q_i)$. Similarly, the combined vector of the Coriolis force, the centrifugal force terms, and the gravity term in our study of the first and third joints is the 2×1 matrix.

$$
\begin{aligned}
V(q',q) &= [V_1, V_2]^T = C(q, q')q' + G(q), \\
V_1 &= -2a_2 q_1' q_3' \sin(2q_3) + 2a_3 q_1' q_3' \cos(2q_3) + a_4 q_1' q_3' \cos(q_3) - a_5 q_1' q_3' \sin(2q_3), \\
V_2 &= 2a_2 (q_1')^2 \cos(q_3)\sin(q_3) - a_3 (q_1')^2 \cos(2q_3) - 0.5a_4 (q_1')^2 \cos(q_3) + 0.5a_5 (q_1')^2 \sin(q_3) \\
&\quad + a_7 \sin(q_3) + a_8 \cos(q_3).
\end{aligned} \tag{5}
$$

Equation (5) is substituted into Eq. (1) to obtain the following general kinetic equation:

$$M(q)q'' = V(q, q') + d = \tau. \tag{6}$$

In this paper, $X_1 = q = [q_1, q_3]$ and $X_2 = q' = [q_1', q_3']$ are the state variables, then the state space expression of the PHANTOM Omni CLMR dynamic equation is defined as

$$\begin{cases} X_1' = X_2, \\ X_2' = M^{-1}(\tau - d - V(q,q')). \end{cases} \tag{7}$$

3.2 Dynamic model of CLMR

The mobile device of the CLMR consists of two driving wheels and two training wheels as shown in Fig. 2. Forward power is provided by the rear wheels and the direction is controlled by steering the front wheels. In a system composed of N CLMRs and one PHANTOM Omni controller, the kinematic model of the ith CLMR can be expressed as

$$\begin{bmatrix} \dot{x}_i \\ \dot{y}_i \\ \dot{\phi}_i \\ \dot{\theta}_i \end{bmatrix} = \begin{bmatrix} \cos\phi_i \\ \sin\phi_i \\ \tan(\theta_i / L) \\ 0 \end{bmatrix} \cdot v_i + \begin{bmatrix} 0 \\ 0 \\ 0 \\ 1 \end{bmatrix} \cdot \omega_i. \tag{8}$$

Unlike a differential mobile robot, the steering angular velocity of a CLMR is related to the forward velocity and spot steering cannot be realized. The nonholonomic constraints in the moving process for the CLMR can be expressed as

$$\begin{cases} \dot{x}_i \sin\phi_i - \dot{y}_i \cos\phi_i = 0, \\ \dot{x}_i \sin(\phi_i + \theta_i) - \dot{y}_i \cos(\phi_i + \theta_i) - L \cdot \dot{\phi}_i \cos\theta_i = 0. \end{cases} \tag{9}$$

The motion of the CLMR is mainly controlled by longitudinal traction and the steering force. Considering that the steering angle of the front wheel is usually relatively small in actual operation, its dynamic model can be expressed as

$$\begin{cases} m_i \cdot \dot{v}_i = \tau_{vi} - F_{ui} \cdot \cos\theta_i - F_{wi} \cdot \sin\theta_i + \tau_{di}^v(v_i, t), \\ J_i \cdot \dot{\omega}_i = \tau_{wi} + F_{wi} \cdot L_i \cdot \cos\theta_i + \tau_{di}^w(\omega_i, t) + c_\theta \cdot \tan\theta_i \cdot \sec^2\theta_i \cdot v_i^2, \\ c_\theta = \dfrac{m_i + J_b + 4J_v}{L^2} + \dfrac{J_h}{r^2}, \end{cases} \tag{10}$$

where τ_{vi} is the traction force; τ_{wi} is the torque applied on the steering wheel; F_{ui} is the friction force in the forward direction; F_{wi} is the transverse force, both $\tau_{di}^v(v_i, t)$ and $\tau_{di}^w(\omega_i, t)$ are the sum of other friction forces and external interference; J_i, J_b, J_v, and J_h are the uncertain inertia coefficients in the system, which are related to the parameters of the CLMR; and r is the wheel radius.
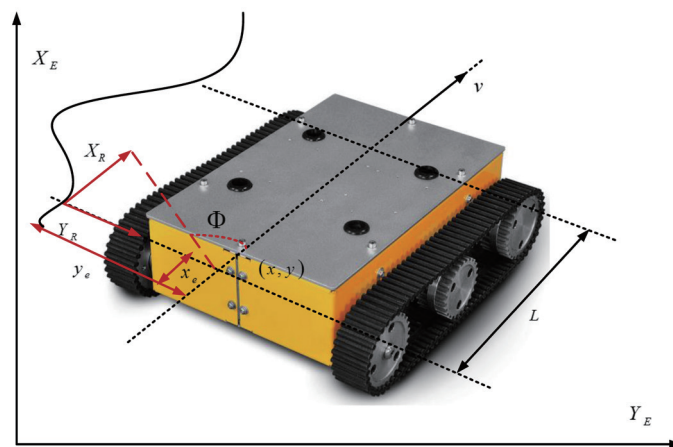
Fig. 2.   (Color online) Structure of CLMR.

4.   Improved Smith Predictor

4.1   Improved Smith predictor

A schematic diagram of control optimization with the Smith predictor method is shown in Fig. 3. The predictor consists of a given regulator, a load regulator, and a system model. In Fig. 3, $R(s)$ is the input, $D(s)$ is the load disturbance, $G_p(s)e^{-\tau_d s}$ is the transfer function of the controlled object, $e^{-\tau_d s}$ is the pure delay link, and τ_d is its delay time. The system model is made up of a nondelay model $G_p^*(s)$ and an equivalent delay time τ_d^*. To ensure that the system output response has no residual difference, both regulators are proportional integral (PI) action regulators, i.e.,

$$G_{CJ}(s) = K_{CJ}\left(1 + \frac{1}{s \cdot T_{CJ}}\right), J = 1, 2, \tag{11}$$

where K_{CJ} is the proportional gain and T_{CJ} is the time constant. This algorithm differs from the original Smith algorithm in that the given response and load response of the closed-loop system are uncoupled and are tuned by two separate PI regulators $G_{C1}(s)$ and $G_{C2}(s)$, respectively.

The controlled object consists of a first-order link and a delay link, and the transfer function is defined as

$$G_p(s)e^{-\tau_d s} = \frac{K_p}{1 + s \cdot T_p}e^{-\tau_d s}, \tag{12}$$

where K_p is the system gain and T_p is the time constant. Then the transfer function of the system model is
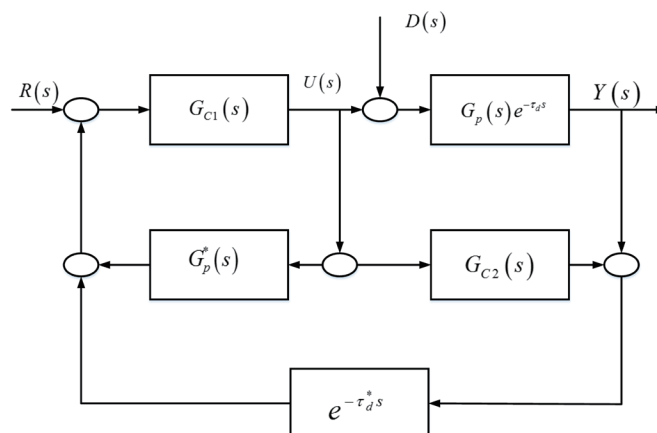
Fig. 3.   Schematic diagram of Smith predictor control optimization.

$$G_p^*(s)e^{-\tau_d^* s} = \frac{K_p^*}{1+s \cdot T_p^*}e^{-\tau_d^* s},$$ (13)

where K_p^*, T_p^*, and τ_d^* are the estimated values of K_p, T_p, and τ_d, respectively. For example, if $G_p^*(s) = G_p(s)$ and $\tau_d^*(s) = \tau_d(s)$, then the transfer function $W_r(s)$ and load disturbance function $W_d(s)$ of the system are

$$\begin{cases} W_r(s) = \dfrac{K_{C1} \cdot K_p \left(s \cdot T_{C1}+1\right)e^{-\tau_d s}}{s \cdot T_{C1}\left(s \cdot T_p +1\right)+K_{C1}\cdot K_p\left(s \cdot T_{C1}+1\right)}, \\[4mm] W_d(s) = \dfrac{K_p \cdot T_{C2}\cdot e^{-\tau_d s}}{s \cdot T_{C2}\left(s \cdot T_p +1\right)+K_{C2}\cdot K_p\left(s \cdot T_{C2}+1\right)e^{-\tau_d s}}. \end{cases}$$ (14)

If the system model is ideal, and therefore the input and load responses can be independently controlled, i.e., $G_{C1}(s)$ and $G_{C2}(s)$ confirm the transfer function $W_r(s)$ and the load disturbance function $W_d(s)$, respectively, then the two controllers can be adjusted separately to improve the tracking and anti-interference performance. Moreover, the system model is not included in the load disturbance part of the algorithm, so the accuracy of the system model does not affect the anti-jamming ability of the load.

4.2   GP algorithm

GP, a prediction method for systems with uncertain factors, can identify the system factors and the development trend of the different degrees in the correlation analysis, process the raw data to find the law by which the system changes, generate data sequences with strong regularity, and then set up a corresponding differential equation model to predict the future trend of the development. In the establishment of the traditional GM (1,1) model, the sequence generated by one summation has the grey exponential rate, and the fitting and prediction accuracy of the GM (1,1) model is determined by the parameters a and b. In the traditional modeling process, the whitening differential equation [Eq. (15)] is estimated by the least squares method.

$$\frac{dx^{(1)}(t)}{dt}+ax^{(1)}(t)=b$$ (15)

The general solution of the whitening differential equation has an exponential form. Here, the known data is first used to perform polynomial fitting to approximate the exponential function, and then a and b are estimated by an algorithm. According to the traditional GM (1,1) modeling process, the solution function of the established whitening differential equation is

$$x^{(1)}(t)=\frac{b}{a}+\left(x^{(0)}(1)-\frac{b}{a}\right)e^{-at}.$$ (16)

The accumulated data $x^{(1)}$ is used to perform polynomial fitting by the least squares method to obtain the polynomial.

$$s(t) = a_1 \cdot t^n + a_2 \cdot t^{n-1} + \cdots + a_{n-1} \cdot t + a_n. \tag{17}$$

By using several polynomial fittings and the general trend of the accumulated data image, multiple polynomial fitting can be achieved. The appropriate order is selected depending on the size of the total relative residual $m = \sum_{k=1}^{n} \varepsilon(k)$. The first derivative of the polynomial $s(t)$ can be defined as follows:

$$y^{(1)}(t) = s'(t) = a_1 \cdot n \cdot t^{n-1} + a_2 \cdot (n-1) \cdot t^{n-2} + \cdots + a_{n-1}. \tag{18}$$

Currently, $\dfrac{dx^{(1)}(t)}{dt} = y^{(1)}(t)$ exists. Therefore, the whitening differential equation can be transformed into $y^{(1)}(t) + a \cdot x^{(1)}(t) = b$. Equation (18) can be expressed in matrix form:

$$Y_n = Bu, \tag{19}$$

where $B = \begin{bmatrix} -x^{(1)}(1) & 1 \\ -x^{(1)}2 & 1 \\ \vdots & \vdots \\ -x^{(1)}(n) & 1 \end{bmatrix}$, $Y_n = \begin{bmatrix} y^{(1)}(1) \\ y^{(1)}(2) \\ \vdots \\ y^{(1)}(n) \end{bmatrix}$, and $u = \begin{bmatrix} a \\ b \end{bmatrix}$. By the least squares method, the estimated value of the parameter column matrix u for which the objective function $J(u) = Y_n - Bu$ reaches a local minimum is obtained as

$$\hat{u} = [\hat{a}, \hat{b}]^T = (B^T B)^{-1} B^T Y_n. \tag{20}$$

The obtained value $\hat{u} = [\hat{a}, \hat{b}]^T$ is substituted into the traditional GM (1,1) model. Then the solution function of the whitening differential equation is defined as

$$\hat{x}(k+1) = \frac{\hat{b}}{\hat{a}} + \left(x^{(0)}(1) - \frac{\hat{b}}{\hat{a}} \right) e^{-\hat{a}t}, \quad k = 0, 1, ..., n-1. \tag{21}$$

5.   Results and Discussion

In this paper, a PHANTOM Omni controller, PC, and CLMR are used to build the entire working system. The composition and signal path of the system are shown in Fig. 4. The PHANTOM Omni controller and the computer use the IEEE1394 serial standard for synchronous
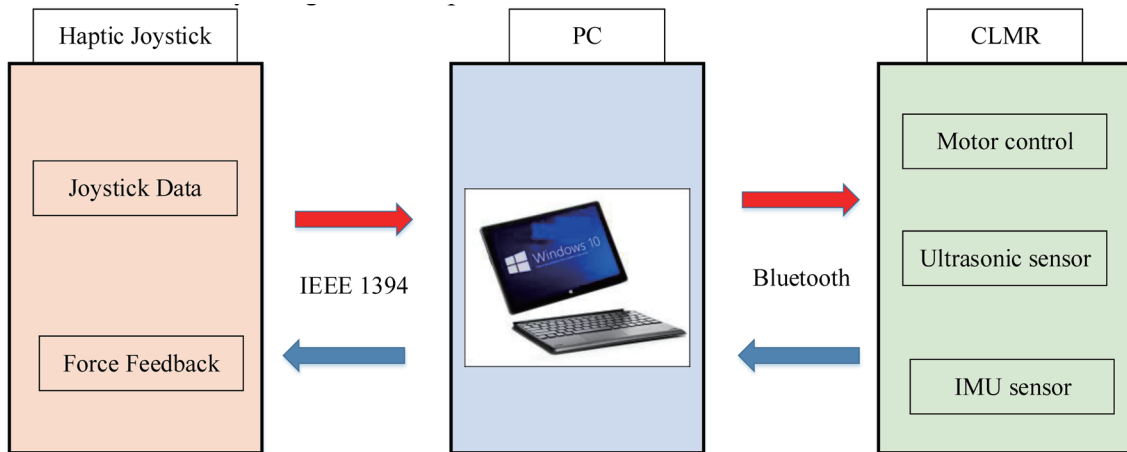
Fig. 4.   (Color online) Block diagram of the entire system.

data transmission, and the CLMR and PC employ a Bluetooth connection. To evaluate the performance of the remote monitoring CLMR system presented in this paper, before applying the GP algorithm to the CLMR operation, the possibility of using the Smith predictor to compensate for the error caused by delay is verified by MATLAB simulation. This simulation experiment is divided into three situations: a remote-control exercise without inserting any time delay (i.e., the most ideal case), the effect after the time delay due to step-by-step insertion, and the remote-control exercise only using the Smith predictor.

5.1   Parameter settings

We assume that the CLMR cluster is composed of the PHANTOM Omni controller and four CLMRs, and the physical parameters selected by the CLMR in the simulation are shown in Table 1. The expected speed for a given manipulator is $v_d = 1.7$ m/s and the expected queue spacing is $p_{ij} = 34$ m. To verify the performance of the CLMR cluster forming the desired queue and moving along the desired path, in the initial state, CLMRs are randomly distributed on both sides of the desired path, and the angle between the initial direction and the starting path point of each CLMR is set to no more than 90º due to the large gyration radius.

Table 1
CLMR parameters.

Parameter	Description	Value
m_i	Mass of CLMR	30 kg
b_i	Distance between rear wheel and center of gravity	0.55 m
L_i	Wheelbase	1.2 m
J	Moment of inertia of wheel	5 kg $\cdot$m^2
v_d	Expected speed	1.7 m/s
p_{ij}	Expected queue spacing	34 m

5.2   Experimental results

To evaluate the performance of the proposed remote monitoring CLMR system, an experimental delay of 0.5 s is introduced in the experiment. We perform three comparative experiments: remote control without any time delay (the optimal case),[15] remote control using only the Smith predictor after the time delay,[16] and remote control using the GP algorithm. The sensor transmits the converted force feedback information to the operator every 0.5 s, and the manipulator uses this information to convey the operation instruction to the CLMR every 0.5 s. The experimental data of the three cases are shown in Fig. 5. The remote-control track without introducing any time delay, marked in red, is smoother than the other tracks, and almost approaches the optimal track in this environment. The uncompensated track in the case of a delay is marked in green. The remote-control track obtained via using the Smith predictor and the GP algorithm system (marked red and blue, respectively) is smooth and the CLMR reaches the destination without colliding with any obstacles.

Figure 6 shows the distance between the CLMR and the obstacle measured in the experiment whose results are shown in Fig. 5. The minimum sensing distance of the ultrasonic sensor is 10 cm and the maximum sensing distance is 50 cm. In the absence of a time delay (marked red), when the distance between the CLMR and the obstacle becomes small, the manipulator responds quickly and adjusts the course, making the journey smooth and short. However, in the case of using only the Smith predictor (marked black), even though the CLMR is close to the obstacle, the manipulator cannot respond quickly and the CLMR remains below the minimum distance from the obstacle (10 cm) for a long time, thus increasing the collision probability and the running time. With the insertion of a time delay, when using the system based on the proposed algorithm (marked green), the CLMR can always maintain an effective distance from the obstacle, allowing the running direction of the CLMR to change smoothly and ensuring a relatively short running time.
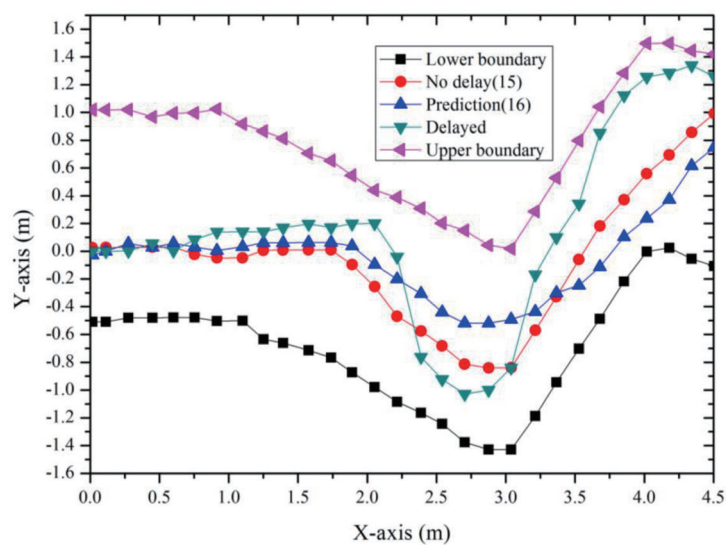
Fig. 5.   (Color online) Trajectory of CLMR in nonlinear motion.
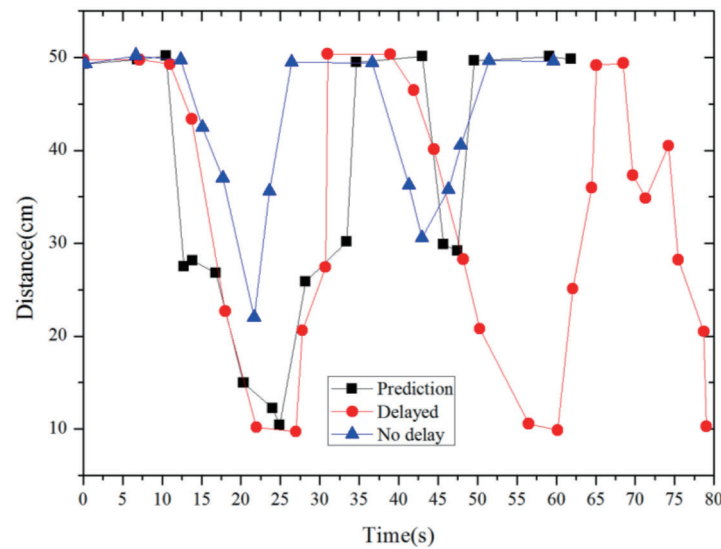
Fig. 6.   Distance between object and CLMR.

6.   Conclusions

In this paper, the problem of CLMR formation control with model uncertainty and an unknown external disturbance is studied. A remote-control system for a CLMR based on the GP algorithm is proposed. To reduce the positioning error caused by an additional delay, the Smith predictor is used to compensate for the additional delay between the PHANTOM Omni controller and the CLMR. At the same time, to reduce the disoperation caused by the additional delay, the GP model is used to predict the values of sensors on the CLMR. The simulation and experimental results show that the system using the Smith predictor and GP algorithm has a good compensation effect on the error caused by the time delay in a nonvisual environment with a time delay. This method is helpful for handling the time delay in various communication methods and communication environments. Because the GP algorithm only changes the internal control algorithm without changing the communication device and environment, it can be used in control, human–computer interaction, and other fields.

References

1   Z. Lei and G. Chen: Ocean Eng. **95** (2015) 78. https://doi.org/10.1016/j.oceaneng.2014.12.001
2   H. Kwon, D. Cha, J. Seong, J. Lee, and W. Chung: Sensors **21** (2021) 4828. https://doi.org/10.3390/s21144828
3   G. S. Kumar, R. S. D. Wahidabanu, and K. G. A. Raajesh: Indian Chem. Eng. **53** (2011) 261. https://doi.org/10.1080/00194506.2011.670934
4   K. Kirtania and M. A. A. S. Choudhury: J. Process Control **22** (2012) 612. https://doi.org/10.1016/j.jprocont.2012.01.003

5   M. Bolignari, G. Rizzello, L. Zaccarian, and M. Fontana: IEEE Rob. Autom. Lett. **6** (2021) 2970. https://doi.org/10.1109/LRA.2021.3062310

6   Z. Hu, Z. Li, C. Dai, X. Xu, and Q. Su: IEEE Access **8** (2020) 84162. http://doi.org/10.1109/ACCESS.2020.2992116

7   X. Xiao, Y. Hu, and H. Guo: J. Syst. Eng. Electron. **24** (2013) 445. https://doi.org/10.1109/JSEE.2013.00053

8   A. Zhang, L. Chong, and W. Bi: Chin. J. Aeronaut. **29** (2016) 1385. https://doi.org/10.1016/j.cja.2016.04.023

9   A. H. Qureshi and Y. Ayaz: Autonomous Robots. **40** (2016) 1079. https://doi.org/10.1007/s10514-015-9518-0

10 A. Vukadinovi, J. Radosavljevi, A. orevi, M. Proti, and N. Petrovi: Sol. Energy **224** (2021) 1426. https://doi.org/10.1016/j.solener.2021.06.082

11 H. Yin, Y. Wang, L. Tang, X. Ding, and R. Xiong: IEEE Trans. Intell. Transp. Syst. **22** (2021) 837. https://doi.org/10.1109/TITS.2019.2961120

12 X. Zhong, X. Zhong, and X. Peng: Neurocomputing **151** (2015) 268. https://doi.org/10.1016/j.neucom.2014.09.043

13 C. Hwang and N. Chang: IEEE Trans. Fuzzy Syst. **16** (2008) 97. https://doi.org/10.1109/TFUZZ.2006.889935

14 H. Wang and Y. Chen: Acta Autom. Sin. **34** (2008) 445. https://doi.org/10.3724/SP.J.1004.2008.00445

15 C. L. Hwang: IEEE/ASME Trans. Mechatron. **21** (2016) 1801. https://doi.org/10.1109/TMECH.2016.2553050

16 K. Majd, M. Razeghi-Jahromi, and A. Homaifar: IEEE/CAA J. Autom. Sin. **7** (2020) 39. https://doi.org/10.1109/JAS.2019.1911816

17 S. Rathinam, S. G. Manyam, and Y. Zhang: IEEE Rob. Autom. Lett. **4** (2019) 391. https://doi.org/10.1109/LRA.2018.2890433

18 L. Xu, W. Zhuang, G. Yin, C. Bian, and H. Wu: IEEE Trans. Veh. Technol. **68** (2019) 11551. https://doi.org/10.1109/TVT.2019.2941396

19 A. Sadowska, T. van den Broek, H. Huijberts, N. van de Wouw, D. Kostić, and H. Nijmeijer: Int. J. Control Autom. Syst. **84** (2011)1886. https://doi.org/10.1080/00207179.2011.627686

20 G. Tang, J. Zhuang, J. Zou, and L. Wan: Ocean Eng. **232** (2021)109147. https://doi.org/10.1016/j.oceaneng.2021.109147

About the Authors

Mingcan Xu received his B.S. degree from Chongqing Three Gorges University, China, in 2003. He was a visiting scholar in Singapore Nanyang Polytechnic, Singapore, and Technical University of Dresden, Germany, in 2013 and 2019, respectively. He joined Chongqing Three Gorges Vocational College in 2003, where he is currently an associate professor. His research interests include electronic information engineering, applications of electronics and communication engineering, and automation. (120731992@qq.com)

Tao Huang received his B.S. degree in electronic information engineering from Chongqing Technology and Business University, China, and his M.S. degree in electronic and communication engineering from Chongqing University of Posts and Telecommunications, China, in 2005 and 2013, respectively. He was a visiting scholar focusing on applications of electronics at Chongqing University and on communication engineering and electrical, media, and information technology at Technische Hochschule Deggendorf (Deggendorf Technical University) in 2015 and 2018, respectively. He is currently an associate professor at the School of Intelligent Manufacturing, Chongqing Three Gorges Vocational College. His research interests include electronics, communication, and automation. (13884897@qq.com).